

Breaking Diffusion with Cache: Exploiting Approximate Caches in Diffusion Models

Desen Sun, Shuncheng Jie, and Sihang Liu
University of Waterloo

Abstract

Diffusion models are a powerful class of generative models that produce content, such as images, from user prompts, but they are computationally intensive. To mitigate this cost, recent academic and industry work has adopted approximate caching, which reuses intermediate states from similar prompts in a cache. While efficient, this optimization introduces new security risks by breaking isolation among users. This work aims to comprehensively assess new security vulnerabilities arising from approximate caching. First, we demonstrate a remote covert channel established with the cache, where a sender injects prompts with special keywords into the cache and a receiver can recover that even after days, to exchange information. Second, we introduce a prompt stealing attack using the cache, where an attacker can recover existing cached prompts based on cache hit prompts. Finally, we introduce a poisoning attack that embeds the attacker’s logos into the previously stolen prompt, to render them in future user prompts that hit the cache. These attacks are all performed remotely through the serving system, which indicates severe security vulnerabilities in approximate caching.

1 Introduction

Over recent years, generative models have developed rapidly. Among them, text-to-image diffusion models dominate image generation in commercial systems, such as those from Google [53], Adobe [1] and OpenAI [44]. Thanks to their remarkable ability in generating high-quality images, users leverage them for scene and character designs [6, 7, 13, 16, 22, 35, 60, 69, 74], artwork construction [66], and advertisement [12]. Users only need to provide their prompts that describe the task, and the diffusion model can generate the image as specified.

Although diffusion models are powerful, they suffer from a high computational overhead. It takes seconds to generate a single image. Such overhead mainly comes from the computation pattern, where a sequence of denoising steps are applied to an initial noise to convert it to the final image. Therefore, reducing the number of steps is a key approach to saving computation. Caching is a promising technique that has attracted attention from both academia and industry [2, 48, 73, 81]. For instance, Pinecone [48] and Zilliz [81] use semantic caches to reuse existing results if a previous prompt aligns with the current one. Approximate cache is another type of optimization [2, 73]. Instead of directly reusing the

prior generations, it reuses intermediate states from similar prompts in the diffusion execution, and resumes the denoising steps to save computation while achieving better text-image alignment. For instance, NIRVANA [2] from Adobe is an approximate cache for diffusion models.

With the widespread use of text-to-image diffusion models, adversaries also exploit these models for their malicious purposes. Some studies take advantage of the diffusion model as a secret channel, embedding private messages and transmitting the output images [8, 24, 37, 47, 76]. Another type of attack steals high-quality prompts to save the prompt design cost [10, 58, 72]. There are also adversaries who aim to poison the diffusion model and inject specific objects or concepts into output images [11, 18, 21, 43, 46, 56, 67, 71].

However, existing attacks focus on the model, while vulnerability from the diffusion model serving system remain largely underexplored. Approximate cache is promising in improving the efficiency of diffusion models, but it introduces additional components to the image generation system, potentially widening the attack surface. The goal of this work is to comprehensively assess the security implications of approximate caching and exploit its vulnerabilities.

To analyze approximate cache, we take NIRVANA [2], the state-of-the-art approximate cache from Adobe by replicating their design, and deploy two widely used text-to-image diffusion models, FLUX [28] and Stable Diffusion 3 (SD3) [14], and two real-world prompt datasets, DiffusionDB [70] and Lexica [58]. The serving system is deployed on cloud GPUs to make the environment realistic. Similar to conventional caches, like those in CPUs or file systems, approximate cache reduces the image generation latency. Our evaluation shows that cache hit or miss latency can be clearly distinguished. Even 10 % steps fewer will bring 0.92 s and 0.48 s lower latency when executed on H100 GPU for FLUX and SD3, respectively. This timing difference can be leveraged by an attacker to determine whether their prompt hits or misses the cache, which we refer to as *Attack Primitive 1*.

However, an approximate cache system is different from conventional caches. Unlike a conventional cache, where every access hits a specific entry, a request hit an entry in an approximate cache depends on prompt similarity, which largely varies by prompts. Thus, even an attacker may probe the cache and receive a cache hit, the output cannot be directly used to derive cached content. We find that the generations from caches have higher similarity, as they preserve part of the original content, such as structure and layout.

Therefore, such similarity can be leveraged to determine whether two cache hits originate from the same cache. We refer to this characteristic as *Attack Primitive 2*.

Based on these attack primitives, we present three attacks. In these attacks, we assume an attack model where the attacker can only access the serving system like normal uses, and does not have prior knowledge about any user prompts in the cache.

First, we demonstrate a remote covert channel, where the sender and receiver exchange messages through a diffusion model service with approximate caching (Section 4). Using special keywords and markers, the sender injects special prompts to the cache. Afterward, the receiver probes the cache to detect whether the sender’s prompts exist. The receiver use a combination of generation timing (Attack Primitive 1) and image content detection (Attack Primitive 2) to confirm that the cache was injected by the sender. Cache hits and misses are encoded as 1s and 0s. Using a number of keywords, the sender can transmit a message with 97.8% accuracy rate under the FLUX model [28]. Using real-world prompt traces from DiffusionDB, we demonstrate that sender’s prompts stay in the cache for over 44 hours, making this channel stealthy.

Second, we perform a prompt stealing attack, CacheTransparency (Section 5). The attacker probes the approximate cache and applies Attack Primitives 1 and 2, leveraging both timing information to determine whether probing prompts hit the cache and structural similarity of generated images to identify which probing prompts map to the same cache. These prompts are then used to recover the target prompt. We evaluate this attack on FLUX and SD3, and two datasets, DiffusionDB and Lexica, with real user prompts. The results indicate that the attacker’s stolen prompts have an average of 0.78 cosine similarity compared to the original ones.

Lastly, we demonstrate a CachePollution attack where an attacker can inject their content (i.e., logos in this attack) in the diffusion model’s cache, and poison other users’ generations (Section 6). The attacker first employs an embedding-space logo injection model to seamlessly embed the logo in stolen prompts, ensuring a high hit rate by other users. After that, if a user hits the attacker’s cached prompt, the output image will include the logo, even though it is not specified in the prompt.

We summarize the contributions as the following:

- To the best of our knowledge, this is the first work that exploits security vulnerabilities in the approximate cache for text-to-image diffusion models.
- We demonstrate a remote covert channel through an approximate caching system, leveraging images generated by special words to secretly exchange information.
- We design a prompt stealing attack, CacheTransparency. Without requiring users’ output images, the attacker can infer user prompts in the approximate cache.

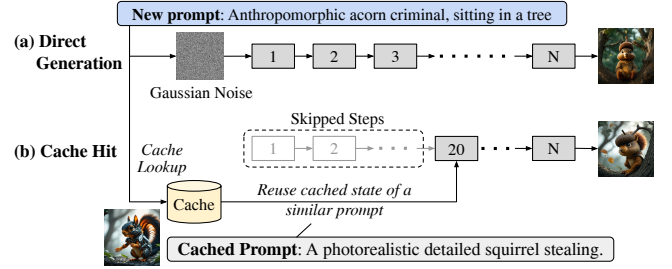


Figure 1. Diffusion model generation (a) directly from Gaussian noise and (b) from an approximate cache.

- We introduce a poison attack, CachePollution. Without manipulating the model or training dataset, the attacker can poison the output of user prompts with specific logos.

2 Background

In this section, we introduce the architecture of text-to-image diffusion models and a key optimization to diffusion models using approximate caching.

2.1 Text-to-Image Diffusion Models

Diffusion model is a probabilistic model of unsupervised learning [19]. During inference, a text-to-image diffusion model takes a Gaussian noise image as input, predicts and eliminates noise by a number of steps, and eventually generates a high-quality image. Figure 1a demonstrates how the diffusion model generates an image with a given prompt. The diffusion model processes the initial Gaussian noise for multiple denoising steps. In each step, it predicts the potential noise and eliminates such noise from the input. The prompt is used to guide the noise prediction in every step. After a number of denoising steps, the noise will finally be recovered to a high-quality image.

2.2 Approximate Cache Serving System

A fundamental challenge of diffusion models is their substantial computational cost, primarily stemming from the iterative denoising process. Inspired by semantic caching in large language models (LLMs) [4, 17, 30, 39] and diffusion models [5, 48, 81] which reuses outputs from prior prompts in subsequent responses, recent work has introduced approximate cache that reuse intermediate states from previous generations [2, 59, 73], achieving a balance between quality and efficiency. The central insight of approximate caching is that similar prompts yield similar outputs. Thus, the intermediate state from a prior, similar request can serve as the starting point for a new request, allowing the system to skip already completed denoising steps. Prior work demonstrates that up to 50% of denoising steps can be reused without noticeable quality degradation [2], with every 10% of steps cached to enable flexible reuse across varying similarity levels. The

more similar the incoming request and the cache are, the more steps the new request can skip.

Figure 1b illustrates how an approximate cache works. When a new prompt arrives, the serving system first compares it with the cache. Existing approximate caching systems usually deploy CLIP [49] to convert the prompt to an embedding and calculate the cosine similarity between the new request and the existing caches. If the similarity score exceeds a threshold, the system considers this as a hit and the request will reuse the corresponding cache. Prior work has shown that a similarity over 0.65 [2] can be regarded as a hit. The new request will continue with denoising steps from the middle and skip the prior steps (20 steps in Figure 1b).

Moreover, cache management also plays a critical role in the effectiveness of approximate caching. In Adobe’s NIRVANA system [2], a prompt is inserted into the cache whenever no existing cache entry is hit. To evict stale entries, NIRVANA employs a Least Computationally Beneficial and Frequently Used (LCBFU) policy, which removes cache items that provide minimal computational savings and are infrequently reused. In contrast, more recent work adopts simpler strategies such as FIFO, ensuring that recently accessed prompts remain available in the cache [73].

3 Vulnerabilities of Diffusion Models

In this section, we discuss the existing attacks on diffusion models and the new security implications due to caching.

3.1 Attacks on Diffusion Models

Although powerful in generating content, recent work has shown that diffusion models have security concerns. One category of attacks notices that the diffusion model’s output inherently contains massive information, making it easy for steganography. Previous studies have demonstrated attack techniques that embed secret messages into images [8, 24, 37, 47, 76]. These attacks usually require an attacker-controlled model to manipulate generated images. Another category of attacks aims at recovering prompts that generated a certain image, as the engineering of prompts is critical in generation. These attacks convert the generated images back to prompts [58] by taking publicly available generated images (e.g., those posted on the internet) as input and training a model to enable recovery. Some attacks also attempt to manipulate the generated content, such as inserting the attacker’s brand information or bias to the model to guide the generation process [11, 18, 21, 43, 46, 67]. Users will receive images with such an injection. Typically, attackers enable such attacks by polluting the training data [8, 23, 43].

3.2 New Vulnerabilities from Caching

Although approximate caching is a promising optimization approach, it introduces an additional component to the diffusion model serving system, which stores and reuses prior

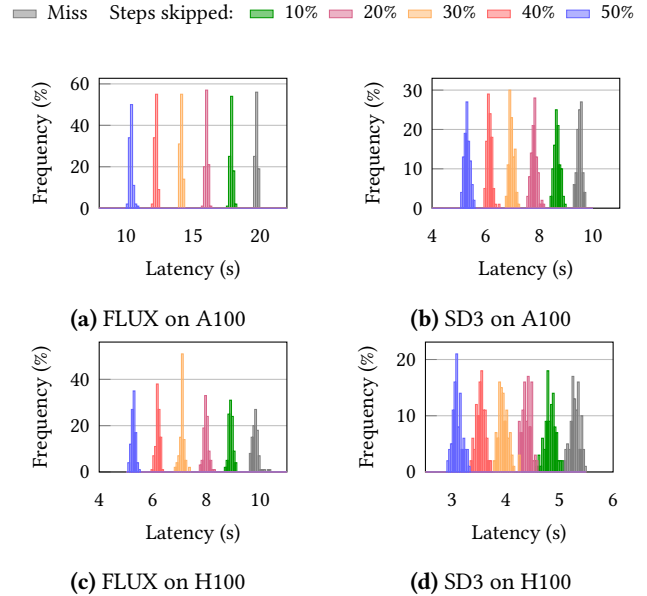


Figure 2. Approximate cache latency distribution ($n = 100$).

prompts, potentially extending the attack surface. Therefore, the goal of this work is to analyze and assess the security risks associated with approximate cache on diffusion models.

3.2.1 Timing of Approximate Cache. Similar to caches in file systems or processors, approximate caching for diffusion models also aims at reducing execution latency. We first analyze the latency distribution with diverse computation savings to better understand its security implications.

To evaluate the latency of approximate caching, we set up a text-to-image diffusion serving system on a remote server using Runpod cloud [51]. The server is over 600 km away from our client, ensuring a realistic cloud serving connection. We implement NIRVANA [2], the state-of-the-art approximate cache from Adobe, as the target serving system. We follow its configuration that caches every 10% of the denoising steps until 50%. We evaluate two most popular commercial open-sourced diffusion models, Stable Diffusion 3 Median (SD3) [14] and FLUX [28, 29] with two types of GPU, A100 and H100 (both have 80 GB of memory). Both diffusion models have 30 denoising steps.

For each model and GPU type, we randomly select 100 prompts and send requests from our local PC to reflect the impact of network fluctuation. Each request is evaluated with different skipped steps. Figure 2 shows the latency distribution. In comparison, the deviation of H100 results is more significant than A100, owing to its faster generation, amplifying the impact of network fluctuation. Nonetheless, on both platforms, skipping even just 10% of the steps yields a clear latency reduction, indicating the feasibility of a timing channel. In the rest of this paper, we use H100 for the

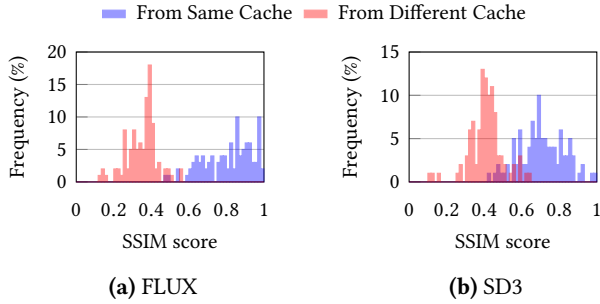


Figure 3. SSIM distribution ($n = 100$).

experiments as it is a more challenging platform for timing channels.

Attack Primitive 1

Since an approximate cache can reduce the generation latency of cache hits, it enables attackers to determine whether their prompts hit any cache.

3.2.2 Similarity of Generation. A cache hit reuses an intermediate result from a prior prompt. Therefore, such reuse likely retains information from the previous generation in the new generation. According to previous studies, the diffusion model determines the image’s layout at an early stage [2, 73, 78], indicating the diversity reduction caused by reusing the same cache. Although the details may change after multiple denoising steps, the structure of the images remains and will demonstrate high similarity compared to the cache. Therefore, we next analyze the similarity distribution for images generated with or without caches.

We evaluate such similarity by generating 100 images from different caches and measuring their Structural Similarity Index Measure (SSIM), which is a common metric to measure the similarity between two images. We evaluated both SD3 and FLUX models. Figure 3 shows the distribution of SSIM scores between two images. If two prompts hit the same cache, their SSIM tends to be higher compared to those that hit different caches. The difference is more prominent in FLUX, as it is a more powerful model that constructs the layout clearly at very early stages, leading to a much higher SSIM score than SD3 when requests hit the same cache.

Attack Primitive 2

Images generated from the same approximate cache have higher similarity. Attackers can use the generated image to infer the original prompt their own prompt hits.

4 Remote Covert Channel

A covert channel is a secret channel for two parties to exchange secret messages. In this section, we demonstrate that a sender and a receiver can establish a remote covert channel

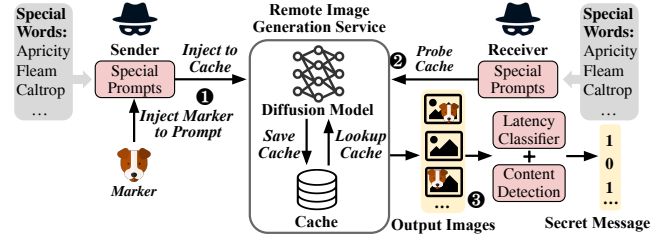


Figure 4. The setup of the remote covert channel based on approximate cache in diffusion models.

through the approximate cache of text-to-image diffusion models, by sending special prompts to leave a message in the cache and retrieving it later.

4.1 Attack Model

We assume that the image generation service deploys the approximate caching technique for better efficiency. When a user sends a prompt, the service caches the prompt and intermediate states of the generation. We assume that the sender and the receiver do not have direct communication channels. Instead, they can only access the same remote diffusion-model-based image generation service through prompts. The sender and the receiver also do not have any knowledge about the existing cached prompts.

4.2 Covert Channel Design

Establishing a covert channel requires accurate identification of whether a prompt hits a cache that was left by the sender. Attack Primitive 1 indicates that a prompt that hits a previous prompt can be identified through its image generation latency. As an approximate cache contains cached prompts from various users, it is difficult to determine whether the cache that the receiver’s prompt hits is left by the sender. Therefore, we use a special keyword (e.g., uncommon words) to differentiate the sender’s prompt, which the receiver can use to retrieve the cache. However, the approximate cache may treat a prompt as a hit if another prompt is similar to other parts of the receiver’s prompt, even if the sender did not inject such a prompt to the cache. Attack Primitive 2 indicates that the output image can be used to infer the original cache, as they have higher similarity than other generated images. Based on these attack primitives, we additionally include a special marker. When leaving the message, the sender combines the marker with the special keyword in the prompt. Then, the receiver can probe the cache using the keyword and perform a two-level detection to confirm whether the prompt hits a cache (using latency) and whether the hit is on sender’s prompt (by detecting the marker in the output image).

Figure 4 demonstrate the covert channel process. The sender first injects the cache with special keywords (1). Afterward, the receiver sends prompts with the same keywords



Figure 5. Covert channel examples (image generated by FLUX).

②). Then, the receiver uses the two-level detection to determine whether they hit sender’s prompt (③). A hit or a miss transmits a bit of 1 or 0, respectively. Specially, the covert channel has the following components.

Unique prompt generator: We first use an LLM to generate a set of special, ancient words that are no longer used today, without any prior knowledge about the prompts in test dataset. These special words are preknowledge shared by the sender and the receiver (e.g., shared offline before transmission). Then, both the sender and receiver use an LLM to construct prompts. On the sender side, the Llama model constructs a prompt for each special word with the marker. On the receiver side, the Llama model constructs a prompt for each special word to probe the cache.

Latency classifier: The receiver profiles the generation latency of the serving system and uses the average latency of hit and miss cases to build a classifier that determines whether their probing prompt hits any cache.

Content detector: The receiver uses a content detection model that recognizes the predefined marker in the output image. If recognized, the receiver considers as hitting sender’s prompt.

4.3 Setup

Platform. We use the approximate cache system and cloud platform introduced in Section 3.2.1.

Model and Dataset. We select the state-of-the-art text-to-image diffusion model, FLUX [28], as the primary model for evaluation. We additionally evaluate a smaller model, Stable Diffusion 3 Medium (SD3) [14]. We use DiffusionDB as the main dataset which contains real-world user prompts and use Lexica as a secondary dataset which contains a smaller number of prompts but in different styles. We only choose prompts in English. In practice, other languages can also be used for this covert channel. We configure 100 GB cache size for DiffusionDB and 1 GB for Lexica due to their number of prompts and deploy the same cache replacement policy as NIRVANA [2] as default.

Metric. The success rate depends on two factors:

- **Insertion success rate** measures the rate of successful cache insertion by the sender. If the sender posts a request

but hits the cache, the cache system will not insert a new cache, leading to incorrect message transmission.

- **Detection success rate** measures receiver’s rate of successful retrieval of prompts with special words and the associated detection of the marker, once the sender has injected the special prompts to the cache successfully.

Sender and Receiver Setup. We use a Llama-3 70B model as the LLM to construct 10 special keywords and the corresponding unique prompts. Figure 5 illustrates these keywords and images generated by FLUX for message transmission. These extremely uncommon words increase the chance that the receiver’s prompts hit the sender’s caches. We use “dog” as the marker for FLUX (this example) and “McDonald’s” for SD3. This is because FLUX is a more powerful model that can render complicated objects from the cache compared to SD3. If the receiver does not hit the sender’s prompts, the output images resemble those in the first row; if the sender has inserted their caches, the receiver obtains outputs like those in the second row. DINOv2 [45] is used to detect the marker in receiver’s generated images, which is the same method of object detection in Silent Branding [23]. **Baseline.** We introduce a baseline that only uses generation latency of the prompt with special words to determine cache hit or miss, without using any marker.

4.4 Results

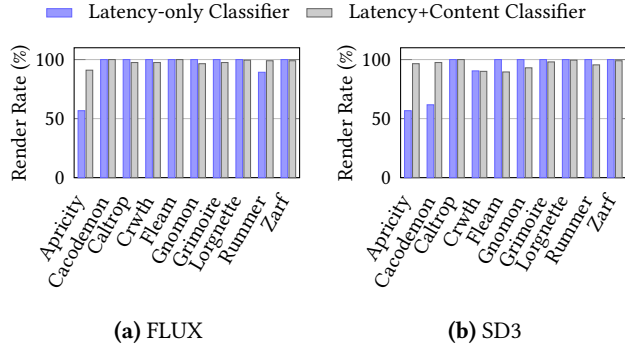
This section presents the evaluation results.

4.4.1 Overall covert channel accuracy. We evaluate covert channel 100 times on both FLUX and SD3. Both sender and receiver send requests to the remote cloud. We assume that the cache system has all the unique prompts from DiffusionDB-2M. Table 1 shows that the covert channel achieves over 97.8% and 95.8% accuracy in FLUX and SD3, respectively. FLUX achieves a higher and more stable accuracy than SD3. This is because FLUX is a more powerful model, capable of generating clearer objects even in early denoising steps. Thus, the cached intermediate states in FLUX are more likely to preserve these objects.

We further explore the accuracy breakdown. Incorrect transmission can potentially come from two sources. First,

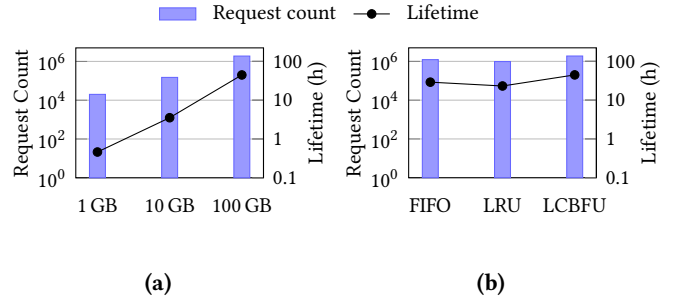
Table 1. Accuracy breakdown ($n = 100$).

Model	Overall Accuracy (Latency + Content Classifier)	Latency-only Classifier
FLUX	97.8 %, $\sigma=2.5$ %	94.6 %, $\sigma=13.0$ %
SD3	95.8 %, $\sigma=3.6$ %	90.8 %, $\sigma=16.1$ %

**Figure 6.** Render success rate of each keyword ($n = 100$).

the sender’s prompt may hit an existing cache, without being cached in the serving system. Consequently, the receiver always receives a bit of 0. Our experiment shows 100 % cache insertion success rate because the sender’s prompts are not similar to either Lexica or DiffusionDB-2M. Second, the latency classifier and content detector in two-level detection can also cause inaccuracies. Table 1 shows the latency classifier’s average accuracy, which is also high (94.6% and 90.8% for FLUX and SD3, respectively) but varies by keyword. Misclassifications occur most often when the sender omits a prompt for a keyword (to transmit a 0), since these prompts are more likely to hit other caches and cause false positives. Figure 6 presents the latency classifier’s accuracy for all 10 keywords. The latency classifier has less than 60 % accuracy for some keywords (e.g., *Apricity*), as the attacker has no knowledge of other users’ data. In contrast, including the content classifier ensures a more consistent accuracy in both models. In a few cases, the content classifier slightly lowers the accuracy because the model fails to render the marker clearly. This is more prominent in the weaker model, SD3.

4.4.2 Lifetime of Sender’s Cache. We evaluate the lifetime of the sender’s cache entries, i.e., how long an injected prompt remains cached before eviction. We follow the same setup as NIRVANA [2], where a prompt is injected only if it does not hit any cache. We replay the trace in DiffusionDB-Large with 14M prompts according to the timestamps and use FLUX as the image generation model. We insert the sender’s prompts once the approximate cache is full, and count the time and number of prompts the generation serves until eviction. Figure 7a shows results under different cache size.

**Figure 7.** Sender’s cache lifetime under (a) different cache sizes (LCBFU) and (b) replacement policies (100 GB cache).

As the cache size increases, the lifetime of injected caches also increases significantly.

Figure 7b shows the lifetime under three replacement policies: LCBFU and FIFO are the default replacement policies in prior approximate caching systems [2, 73]; LRU is a popular replacement policy. We notice that LCBFU keeps the sender’s caches for the longest time because it manages caches in a finer granularity, effectively allowing for more cache entries. LRU performs the eviction earliest, as the attacker’s keywords barely received hits from normal users. Overall, the sender’s prompts last in the cache for a long time (up to 44 hours), making the channel stealthy.

4.5 Discussions

Compare to prior attacks on diffusion model that transmits secret messages [8, 24, 37, 47, 76], our covert channel does not modify or train the diffusion model. Moreover, instead of using the timing channel alone, like remote covert channels on conventional caches [3, 27, 33, 36, 54, 55], this covert channel analyzes the generation output to achieve higher success rate. Another key difference is that this covert channel allows the message to remain cached for days, allowing the receiver to retrieve them at any time before eviction and making the message exchange more covert.

Moreover, even if the timing channel is unstable due to network traffic or delayed response, our covert channel still works owing to the content classifier. The only difference is that the attacker still needs to detect whether the output image contains the marker instead of simply measuring the latency when it fails to hit a cache.

5 CacheTransparency: Prompt Stealing Attack

As prior work has shown, generating high-quality images requires careful design of modifiers [10, 58]. In this section, we introduce CacheTransparency, a prompt stealing attack, where the attacker’s goal is to steal other users’ prompts (e.g., for commercial usage) from the approximate cache to reproduce their image generation.

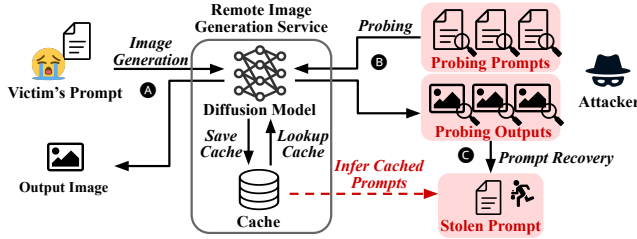


Figure 8. The setup and overview of CacheTransparency attack.

5.1 Attack Model

We assume the same image generation serving system as Section 4.1. Similarly, we assume the attacker has no additional privilege than other normal users, i.e., zero knowledge of other users’ prompts or generated images and they can only send requests to those generation services to get images. The attacker also does not know about the cache size. No matter how many caches are in the cache system, the attack method still identifies one specific cache.

5.2 Attack Design

Figure 8 illustrates an overview CacheTransparency attack. The victim sends a prompt to the image generation service and the prompt is cached (A). The attacker later sends probing prompts to the service (B) and recovers the victim’s prompt by analyzing the probing prompts (C).

Challenges. The attacker can distinguish a probing prompt’s hit/miss through latency (Attack Primitive 1). However, the similarity between the probing prompt and the target prompt can be low (e.g., only 0.65). Thus, a single probing prompt is insufficient for recovery. Using multiple probing prompts should improve the accuracy but two challenges need to be solved. First, it is difficult to determine which cache a probing prompt hits. Approximate caching retrieves prompts by similarity, which introduces uncertainties. A misclassification on the target prompt degrades the recovery accuracy. Second, the embedding space does not directly map to words. Therefore, even with an accurate classification of hits, converting multiple probing prompts that are similar in the embedding space back to the original prompt remains challenging.

Solution. To address these challenges, CacheTransparency follows the approach in Figure 9. First, we design a *prompt constructor* to construct probing prompts (1) and get corresponding images (2). Once the attacker has collected enough probing data, a two-level *classifier* (3) clusters these prompt-image pairs into multiple groups, where probing prompts in the same group hit the same target prompt (4). After that, the attacker uses an *embedding predictor* (5) to guess the cache embedding that every group hits (6). The created embedding maintains high similarity to every prompt in the group. We consider this embedding as the approximation of

the cache and recover it back to the prompt with *prompt recoverer* (7). The recovered prompt is the stolen prompt. The attacker sends these prompts back to the same generation application for the images. We next discuss these components in detail.

Prompt Constructor: The *prompt constructor* generates a batch of prompts by sampling a variable number of modifiers from a predefined modifier collection file. We use the same modifier pool as a prior study [58]. For each attack trial, *prompt constructor* starts from a subject and randomly samples modifiers from the pool. The number of modifiers per probing prompt is diverse. After probing a prompt, we send it to the image generation service and exploit the latency to determine whether this prompt hits a cache. Once we detect a hit, we collect the prompts for the following processing. *Prompt constructor* also leverages a filter to prevent the constructed prompts from being too similar to the hit prompts in order to increase the diversity of the hit prompts, avoiding overfitting when training *embedding predictor*.

Classifier: CacheTransparency’s classifier examines the output of probing prompts from two angles, *timing* of the generation that determines if a prompt hits a cache and *structural similarity* of the outputs that determines which probing prompts hit the same cache. The attacker sends the probing prompts generated by the *prompt constructor* to the image generation service and measures the response latency. Timing classification is based on response latency, the same approach as Section 4.2. Prompts with response time within cache hit latency threshold (9.5 seconds for FLUX and 5.06s for SD3 on H100) are then placed in the *hit set*. As Attack Primitive 2 and Figure 3 have shown, generated images tend to be more similar if they reuse the same cache. To further increase the classifier’s accuracy, Structural Classifier also incorporates the prompts’ CLIP similarity to avoid false positives caused by similar input. Our *structural classifier* is based on a 3-layer MLP, where the input is the CLIP similarity of two prompts and the SSIM scores of the corresponding images, and outputs whether two prompts hit the same cache.

Embedding Predictor: Once the classifier has grouped all probing prompts into a number of groups, the attacker can then convert each group into the original cache that they hit. The *embedding predictor* is an embedding training process with Stochastic Gradient Descent (SGD) algorithm. *Embedding predictor* first creates an embedding (E) randomly, and computes the similarity score (S_E) with other prompts from the same cluster. Theoretically, the cached embedding should keep a high similarity score (S_c) with these prompts. Since we can only get the number of skip steps instead of the accurate similarity score, we assume that the similarity score is the upper bound of the corresponding skip level. The *embedding predictor* sets the Mean Squared Error (MSE) of S_E and S_c as the loss, and updates the embedding E based on the SGD algorithm. Then, it iterates this procedure until E achieves similar similarity as the cache.

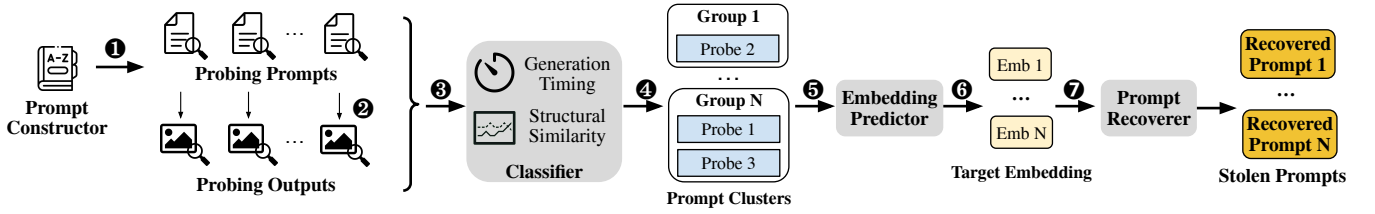


Figure 9. Design details of CacheTransparency attack.

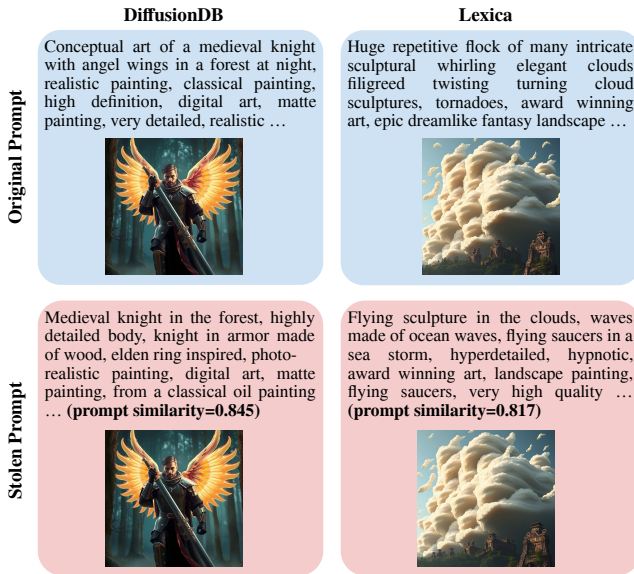


Figure 10. Examples of CacheTransparency.

Prompt Recoverer: The next step is to convert the embedding to prompts. Inspired by prior studies [40], we design a generative model named *prompt recoverer* to recover embeddings to prompts. It first maps an embedding from CLIP embedding space to GPT2 space with an MLP-based model. Afterward, it uses GPT2 [50] to iteratively generate the recovered prompt word by word. When training, we do not freeze GPT2’s parameters to enhance the alignment between the output and normal users’ prompt style.

5.3 Attack Setup

Platform. Like before, we use the approximate cache system in Section 3.2.1.

Model and Dataset. We follow the same diffusion models and datasets as the covert channel, as described in Section 4.3. This attack does not depend on cache replacement, as the attacker only probes the approximate cache. Therefore, we evaluate this attack using a fixed number of cache entries. Due to different dataset sizes, we evaluate 100k cache entries for DiffusionDB dataset while Lexica has 10k.

CacheTransparency Training. CacheTransparency consists of four components as described in Section 5.2. The

prompt recoverer and *classifier* need to be trained. We randomly select 20% prompts in DiffusionDB to train these two models, and evaluate CacheTransparency on the other 80% prompts and the *unseen* dataset Lexica. Specifically, we select 200 unique prompts in the 20% training set as cached prompts, and use other prompts that are similar to these caches to generate images. Using these prompt-image pairs, we train the *classifier* based on their SSIM and CLIP similarities. *Prompt recoverer* takes the CLIP embedding as the input and the original text as the target output.

CacheTransparency Probing. Probing happens in two stages: the first stage constructs the prompts randomly, and exploits the latency classifier to collect the hit prompts. Once the hits exceed a certain number (35 in our evaluation), probing moves to the second phase, where we randomly sample probing prompts whose similarity to the hit prompts falls within an interval (0.5 – 0.6 in our evaluation). This increases the likelihood of hitting the cache while maintaining prompt diversity to recover a more precise prompt.

Accuracy Metrics: We use the following metrics to evaluate the similarity of stolen prompts with the victim’s prompts:

- **Prompt semantic similarity.** The stolen prompt should describe similar content as the target prompt, measured by the cosine similarity in the CLIP embedding space.
- **Image Similarity.** The image generated by the stolen prompt should also be similar to the victim’s original generation. Such similarity is evaluated in terms of the CLIP similarity, pixel-level (PSNR), and structure-level (SSIM).

5.4 Results

Figure 10 displays two examples of CacheTransparency from DiffusionDB and Lexica. The first row shows user prompts and the generated images. The second row shows CacheTransparency’s stolen prompts and the reproduced images. The stolen prompts are also similar to the user’s prompts. Even though there are differences at the word-level, from a model’s perspective, the two prompts are highly similar. Thus, the generated images are almost identical to the original.

5.4.1 Overall Success Rate. We first conduct an experiment to show the prompt and image similarity on both models and both datasets. We process 100 rounds for each configuration and try to recover at least one prompt for each

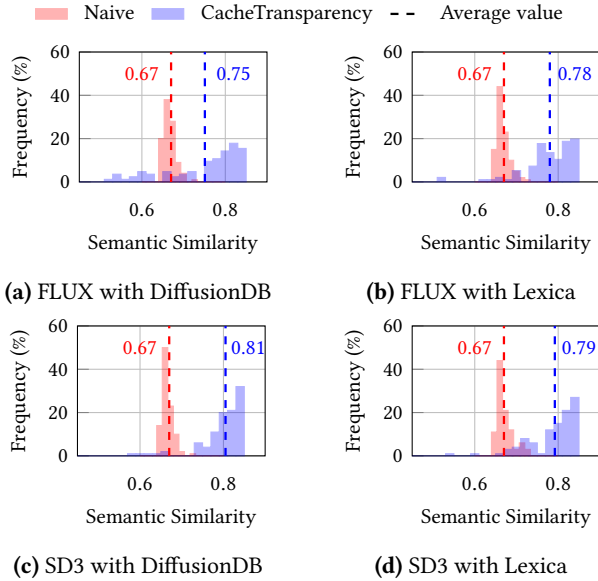


Figure 11. Semantic similarity score distribution ($n = 100$).

Table 2. Image recovery quality of CacheTransparency.

Dataset	Model	Method	CLIP	PSNR	SSIM
DiffusionDB	FLUX	Naive Probing	0.86	20.89	0.74
		CacheTransparency	0.90	24.95	0.82
	SD3	Naive Probing	0.74	15.02	0.55
		CacheTransparency	0.85	19.92	0.75
Lexica	FLUX	Naive Probing	0.88	20.11	0.72
		CacheTransparency	0.95	25.62	0.85
	SD3	Naive Probing	0.75	15.39	0.531
		CacheTransparency	0.84	19.72	0.71

round. Figure 11 shows the distribution of the similarity between the target prompts and the recovered prompts. On average, prompts recovered by CacheTransparency achieve 0.75–0.81 similarity scores, much higher than the naive baseline which is 0.67. According to prior studies, such high prompt similarity can be considered successful [10, 58]. A few prompts recovered by CacheTransparency has a similarity score lower than 0.65 due to false positives from our classifier in those specific cases. We will discuss the impact of the false positives in Section 5.4.3.

Table 2 presents the image similarity compared to the target image. CacheTransparency outperforms the baseline in all three metrics. The PSNR score exceeds 25, indicating negligible loss compared to the target image [15]. The SSIM score also remains at a high level. The baseline’s image similarity in FLUX performs better than SD3, mostly because

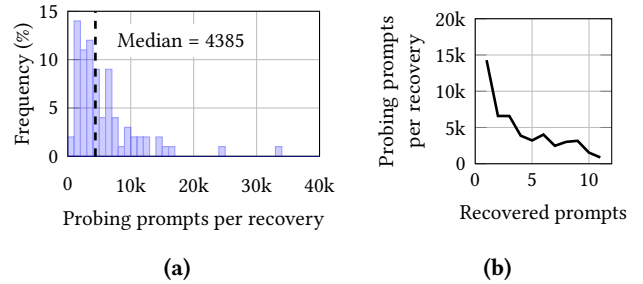


Figure 12. (a) Distribution of probing prompts and (b) amortized probing number over recovered prompts.

FLUX’s early cache contains clearer content than SD3, resulting in more similar output. Nonetheless, CacheTransparency also manifests obvious improvements over the baseline.

5.4.2 Number of Probing Prompts. To steal a prompt, the attacker needs to send a large number of probing prompts before collecting a good number of hits for recovery. Figure 12a shows the distribution of the number of probing prompts per recovery (stolen prompts). Despite a long tail, the median number is 4385 prompts. The high number is mainly due to the first stage of probing; after finding initial hits, the prompt constructor can generate more specific probing prompts in the second stage. Figure 12b shows the median number of probing prompts per recovery over different numbers of recovered prompts in each round of recovery execution. The number of probing prompts is amortized, as the number of recovered prompts in a round increases (as low as 874 when 11 prompts are recovered in a round).

5.4.3 Ablation Study. We explore the effectiveness of CacheTransparency components.

Classifier. We evaluate the effectiveness of the classifier. Because the classifier takes both the prompt and image as input to determine structural similarity, we evaluate both FLUX and SD3 using the main dataset, DiffusionDB. We include two additional methods as comparison points: (a) A greedy method that uses all prompts that hit the cache for recovery, without grouping them by their structural similarity. (b) An ideal scenario that classifies the probing prompts 100% correct. The prompt constructor generates the same probing prompts for CacheTransparency and these methods. Figure 13 shows that CacheTransparency is only 3.01% lower than ideal on average, following similar distributions. In comparison, without considering structural similarity, recovered prompts by the greedy method have a lower similarity (0.69 on average).

A false positive occurs when a probing prompt hits a different cache but is mistakenly classified as hitting the target cache. In our experiment, SD3 and FLUX have 0.36 and 1.63 false positives on average. We further evaluate its impact

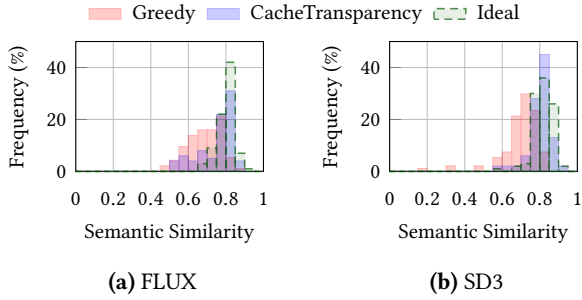


Figure 13. The effectiveness of classifier ($n = 100$).

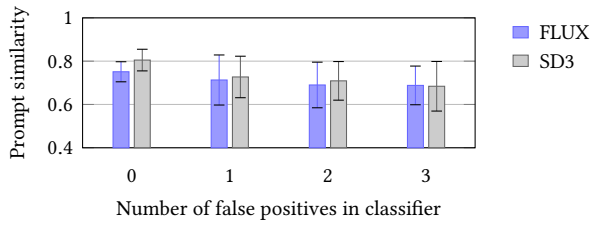


Figure 14. Sensitivity to the false positive in classifier (prompts from DiffusionDB).

by randomly inserting variable numbers of false positive prompts into the ideal scenario. Figure 14 shows that the similarity declines with more false positives. Moreover, the deviation also increases a lot with false positives. The experiment also shows that the similarity drops significantly with only 1 false positive, which highlights the importance of an accurate classifier.

Prompt Recoverer. This component converts embeddings back to prompts. We evaluate the similarity loss during this conversion. We only evaluate FLUX since the model doesn’t affect its accuracy. We compare the embedding of the target cache directly with the *embedding predictor*’s output (before recovery), as well as the embedding after conversion back to the prompt (after recovery). Figure 15 presents the distribution of similarity scores. Compared to the embedding before recovery, *prompt recoverer* only incurs 4.4% similarity loss on average, preserving the similarity.

We also compare our prompt recovery technique to an LLM-based method. We compare the similarity score of prompts recovered using *Embedding Predictor + Prompt Recover* in CacheTransparency with those generated by a Llama-3 70B model [38]. Both CacheTransparency and Llama take the same classify results as input. As Figure 16 illustrated, CacheTransparency achieves 10.4% higher similarity scores than Llama. Worth noting that the recovery models in CacheTransparency are lightweight compared to a 70B LLM, being able to execute on local devices (e.g., a gaming GPU). This low hardware requirement further enhances the stealthiness of CacheTransparency.

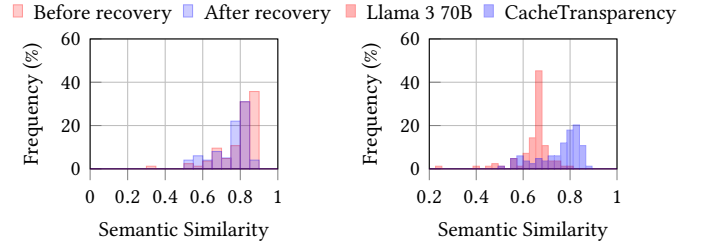


Figure 15. The effectiveness of *prompt recoverer* (FLUX vs. Llama-3 70B (FLUX with DiffusionDB, $n = 100$)).

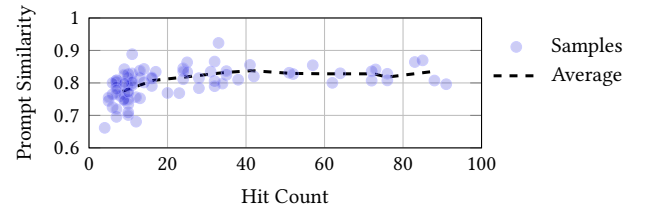


Figure 17. Sensitivity to hit count (FLUX with DiffusionDB).

5.4.4 Sensitivity Study on Hit Count. We analyze the impact of hit count, a key factor in the prompt recovery process, using the primary model, FLUX, and DiffusionDB dataset. We evaluate 100 ideal experiments where the *classifier* is 100% correct and group the experiments by the number of prompts that hit the target cache. Figure 17 presents the curve of the semantic similarity score varied by hit number. Achieving a high similarity score (over 0.8) requires more than 34 hits. When the hit count increases over 26, the recovery similarity plateaus. This indicates that the attacker can stop probing the image generation service once the classifier has collected 26 prompts that hit the same cache.

5.5 Discussions

CacheTransparency is the first prompt stealing attack for text-to-image diffusion models via the approximate cache. Compared to prior works [10, 58, 72], CacheTransparency is able to steal prompts without public images shared by users. This enhances the capability of the prompt-stealing attack. CacheTransparency also constructs multiple probing prompts and exploits timing classifier to determine the hit situation of those prompts, like cache side-channel attacks [20, 26, 32, 34, 62, 64, 65, 75, 77]. Differently, this attack deals with similarity-based cache retrieval, and uses a structural classifier and an embedding predictor to recover the target prompt from a set of probing prompts.

Like the covert channel (Section 4.5), CacheTransparency also works without timing channel in cache. Without timing information, the *structural classifier* can directly cluster the

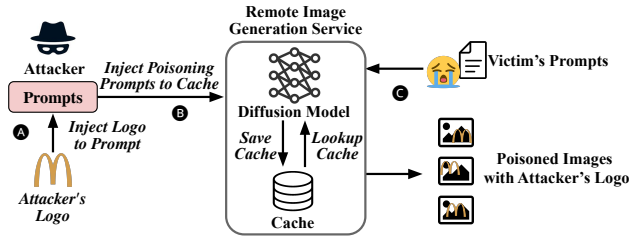


Figure 18. The setup and overview of CachePollution.

prompts by the cache they hit based on the output images. However, this is more costly as the classifier needs to look at each pair of the probing prompts (14k) as input. In contrast, the latency classifier significantly reduces scope of the structural classifier.

6 CachePollution: Image Poisoning Attack

If a prompt hits the approximate cache, the output image resembles the cached one when it is similar with the cache prompt. Therefore, attackers can inject prompts with their preferred information (e.g., logos) to the cache, which will later be reused by victims. In this section, we present an image poisoning attack, CachePollution.

6.1 Attack Model

Figure 18 depicts the setup of this attack. We assume that an image generation service is the same as the previous covert channel (Section 4.1) and CacheTransparency attack (Section 5.1). Likewise, we assume the attacker can only access the image generation service via prompts. The attack’s goal is to inject prompts with information under their control and leave such content in user generations. In this attack, we use logos to demonstrate the attacker’s poisoning capabilities. The injected logos can be used for advertisement purposes.

6.2 Attack Design

Figure 18 illustrates the overview of CachePollution. The attacker first injects the logo into commonly used prompts (A) and then sends these prompts to the approximate cache (B). When a victim hits such poisoned prompts in the cache, the output will display the same logo (according to Attack Primitive 2), even if the victim did not mention it (C).

Challenge. To inject a cache that contains a logo, the logo’s text description needs to be first included in the prompt and then cached. However, directly appending the logo to an arbitrary prompt is less likely to be hit by user prompts.

Solution. Figure 19 depicts the design. First, the attacker steals cached prompts using the CacheTransparency attack (1). These prompts are a good representation of other user prompts and are more likely to be hit. Then, the attacker converts these prompts to embeddings (2) and uses the *logo injector* to embed logo descriptions into the embeddings (3).

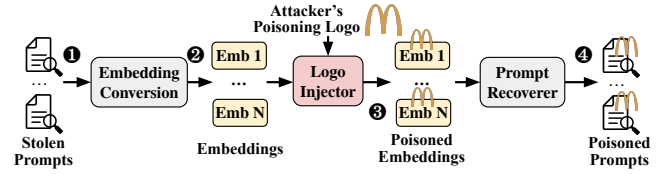


Figure 19. Design of CachePollution attack.



Figure 20. Examples of CachePollution (generated by FLUX).

Afterward, the attacker converts the embedding to a prompt with a similar model as *prompt recoverer* in CacheTransparency (4). This prompt contains the logo but remain similar to the stolen prompt.

Logo injector is the core of this attack, which has two subcomponents: a model for *logo insertion* and another for *embedding prediction*. The *logo insertion* mode is a small attention-based model to combine normal prompts with the attacker’s logos. It takes the prompt embedding and the logo, and generates an embedding that contains both. This is an effective way to insert logos, but the output may have low similarity with the original prompt, making it less likely to be hit by other users. Therefore, we incorporate another *embedding prediction* model to convert the injected prompts to be more similar to the original one. The *embedding prediction model* is similar to the *embedding predictor* in CacheTransparency, except that it includes the logo information. The *embedding prediction model* first creates an embedding (E) and exploits *logo insertion* to guarantee that E has the logo information. We note such an embedding with logo information as E' . Then it computes the similarity score between E' and the original prompt, and trains E' for thousands of steps to make sure E' is almost the same as the original prompt.

6.3 Attack Setup

Platform. We use the same system in Section 3.2.1.

Model and Dataset. Similar to the Convert Channel, we also set FLUX and DiffusionDB as the main model and dataset, and SD3 and Lexica as an extension. To evaluate the poisoning success rate, we send 1M prompts in DiffusionDB-Large

Table 3. Poison effectiveness.

Method	FLUX				SD3			
	DiffusionDB		Lexica		DiffusionDB		Lexica	
	Hit	Render	Hit	Render	Hit	Render	Hit	Render
Direct Inject	2624	1580	1059	744	3408	883	632	139
CachePollution	3646	2104	1226	863	4931	1360	838	180

by their timestamps and the whole Lexica randomly by its default order.

Logos. We evaluate this attack with 6 logos, including 4 well-known logos (“Nike”, “McDonald’s”, “Apple”, “Chanel”) and 2 customized logos (“Triangle”, “Blue Moon”), similar to prior work [23]. We choose 50 target prompts stolen by CacheTransparency. Thus, each logo has 50 poisoned prompts.

CachePollution Training. The *logo injector* model contains a 2-layer MLP and an attention layer. To train this model, we use a training set based on 10 % of DiffusionDB-2M. We randomly insert the logo descriptions into these prompts. The training objective is to maximize the cosine similarity between the model’s predicted embedding and the embedding of logo-inserted prompts. To convert such an embedding back to text, we exploit the same model as *prompt recoverer model* in CacheTransparency. We retrain it with the new dataset which we have added logo descriptions to generate logo text correctly.

Baseline. We take the naive implementation of the poison attack that randomly injects the logo text into the stolen prompts and inserts them into the cache system as a baseline.

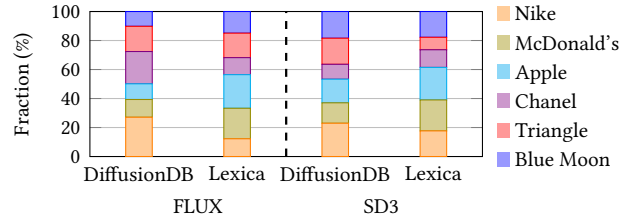
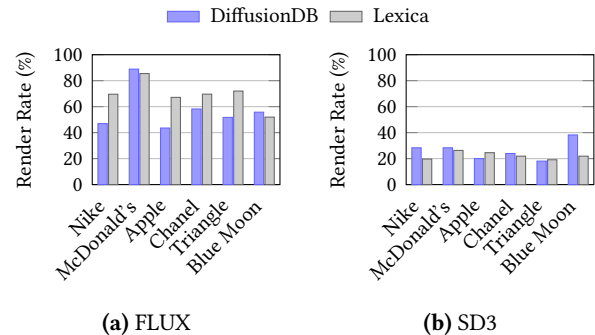
Metric. We use the following metrics to evaluate this attack:

- **Hit Number.** This indicates the number of user prompts that hit the attack’s poisoned cache.
- **Render Rate.** This is the rate of user prompts that hit the cache and contain a visible logo in the output images. The logo is not always rendered successfully by diffusion models, especially when the number of skipped steps is too small or the logo is complicated.

6.4 Results

Figure 20 is an example of the poisoned output (generated by FLUX). The first row presents the images of each logo. The second and third rows show the generated images with and without hitting the poisoned caches. When hitting a poisoned cache, the logo embeds into the generated image.

6.4.1 Poison Success Rate. We first evaluate the hit number and render rate. We simulate user prompts using datasets as described in Section 6.3. In parallel, the attacker sends poisoned prompts periodically to determine whether our cache is inserted successfully based on the generation latency. After that, the attacker generates all the hit images from the poisoned caches, and detects whether the generated

**Figure 21.** Breakdown of hits by logos.**Figure 22.** Render success rate for different models.

images include the logo. The detection model is DINOv2 [45], similar to the method in prior work [23].

As Table 3 illustrates, CachePollution receives more hits than the direct injection baseline in all scenarios, due to the effective *logo injection* method. Consequently, the render rate of CachePollution is also higher. Figure 21 details the breakdown of hits by logos. Because we use the same target prompts for all 6 logos, the variation among logos indicates how well a logo can be blended into the prompt. All 6 logos contribute to the total hit, indicating the generalization of this attack.

We also explore the render rate among 6 logos. Figure 22 demonstrates that FLUX renders logos at a better success rate. In contrast, SD3 struggles to preserve such visual content when reusing the cache. The main reason is that SD3 (Median version) is less powerful than FLUX. As a smaller model, SD3 results in weaker text-image alignment. Even when the logo text is explicitly included in the prompt, SD3 often fails to generate the corresponding logo. Figure 23 illustrates that, when a logo is embedded directly into the prompt, FLUX produces a clear logo, whereas SD3 cannot. Logo complexity also significantly impacts the success rate. For instance, Figure 22b shows that “Triangle” consistently exhibits the lowest render rate with SD3, as its complicated combination of lines can vanish after multiple denoising steps, while “Blue Moon” achieves a high render rate due to its simpler structure.

6.4.2 Sensitivity Study. We then explore CachePollution’s effectiveness under different cache configurations. First, we



Figure 23. Generation comparison between FLUX and SD3 (Median) when the logo is directly embedded into the prompt.

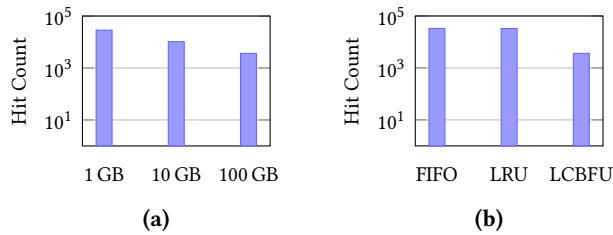


Figure 24. Poison effectiveness under (a) different cache sizes (LCBFU) and (b) replacement policies (100 GB cache).

evaluate the hit count under different cache sizes. Figure 24a shows that the hit count is higher when the cache is smaller, as the target caches get evicted earlier under a smaller cache, allowing more user prompts to hit the attacker’s poisoned cache. Second, we evaluate the hit count under different replacement policies. Figure 24b shows the hit count is higher under FIFO and LRU than LCBFU because the target caches in these schemes get evicted earlier. In LCBFU, caches that were frequently hit in the past are harder to be evicted, leading to a lower hit count.

6.5 Discussion

Unlike previous poison attacks that pollute the training dataset [18, 23, 46, 57, 67], CachePollution poisons a serving system through prompts, without accessing or manipulating the training data. Therefore, this attack assumes a more realistic environment. Moreover, CachePollution can work in combination with other poisoning attacks, further increasing the rendering success rate of the attacker’s content.

CachePollution can also operate without the timing channel. Cache timing is only used for injecting poisoned prompts. Without it, the attacker can analyze the generation to determine whether their poisoned prompt was processed from scratch or a cached prompt, e.g., comparing it with output on a separate system running the same model.

7 Potential Defense Mechanisms

Random cache selection. The approximate caching selects the cache of the highest similarity with the incoming prompt [2, 73], which allows the sender’s prompt with the

same special word to be chosen. The defense mechanism can randomly choose from a number of potential caches. This makes the receiver’s request harder to hit a specific cache entry, significantly decreasing the success rate of the covert channel. Likewise, this also makes CacheTransparency more costly because it requires more probing prompts to collect the same number of hits for each target. For the poisoning attack, fewer prompts will hit the poisoned cache, thus reducing the spread of the attacker’s content.

Content filter. Similar to filters in generative models [31, 61, 63, 68, 80] that defend against not-suitable-for-work (NSFW) content, filters can also be specific to removing the attacker’s content from the cache. For example, to prevent the poisoning attack in this work, the service provider can incorporate a logo filter that detects logo-like objects in the image and potential logo descriptions in the prompt, to make sure both prompts and generated images do not contain logos.

Malicious behavior detector. Stealing cached prompts requires a large number of probing prompts as shown in Section 5.4.2. A malicious behavior detector can monitor user’s activities [9, 25, 41, 42, 52, 79]. When a user appears to abuse the generation system, such as flooding the system with prompts, the service provider can slow down or disable the user’s generation.

8 Conclusions

Approximate caching improves the performance of diffusion models, but it also introduces significant security risks. We demonstrated three such attacks: a covert channel that transmits messages through the approximate cache, a prompt-stealing attack that reveals cached prompts, and a poisoning attack that embeds attacker’s content into user’s generations. These findings demonstrate that approximate caching introduces new security vulnerabilities which must be addressed before widespread adoption.

References

- [1] Adobe. Create with adobe firefly generative AI. <https://www.adobe.com/products/firefly.html>, 2023.
- [2] Shubham Agarwal, Subrata Mitra, Sarthak Chakraborty, Srikrishna Karanam, Koyel Mukherjee, and Shiv Kumar Saini. Approximate caching for efficiently serving Text-to-Image diffusion models. In *21st USENIX Symposium on Networked Systems Design and Implementation (NSDI 24)*, pages 1173–1189, Santa Clara, CA, April 2024. USENIX Association.
- [3] Andrei Bacs, Saidgani Musaev, Kaveh Razavi, Cristiano Giuffrida, and Herbert Bos. DUPEFS: Leaking data over the network with filesystem deduplication side channels. In *20th USENIX Conference on File and Storage Technologies (FAST 22)*, pages 281–296, Santa Clara, CA, February 2022. USENIX Association.
- [4] Fu Bang. GPTCache: An open-source semantic cache for LLM applications enabling faster answers and cost savings. In Liling Tan, Dmitrijs Milajevs, Geeticka Chauhan, Jeremy Gwinnup, and Elijah Rippeth, editors, *Proceedings of the 3rd Workshop for Natural Language Processing Open Source Software (NLP-OSS 2023)*, pages 212–218, Singapore, December 2023. Association for Computational Linguistics.
- [5] Romain Beaumont. Clip retrieval: Easily compute clip embeddings and build a clip retrieval system with them. <https://github.com/rom1504/clip-retrieval>, 2022.
- [6] Aleksey Bokhovkin, Quan Meng, Shubham Tulsiani, and Angela Dai. SceneFactor: Factored latent 3D diffusion for controllable 3D scene generation. In *Proceedings of the IEEE/CVF Conference on Computer Vision and Pattern Recognition (CVPR)*, pages 628–639, June 2025.
- [7] Haoyu Chen, Xiaojie Xu, Wenbo Li, Jingjing Ren, Tian Ye, Songhua Liu, Ying-Cong Chen, Lei Zhu, and Xinchao Wang. POSTA: A go-to framework for customized artistic poster generation. In *Proceedings of the IEEE/CVF Conference on Computer Vision and Pattern Recognition (CVPR)*, pages 28694–28704, June 2025.
- [8] Jiahao Chen, Yu Pan, Yi Du, Chunkai Wu, and Lin Wang. Parasite: A steganography-based backdoor attack framework for diffusion models, 2025.
- [9] Marco Chiappetta, ErKay Savas, and Cemal Yilmaz. Real time detection of cache-based side-channel attacks using hardware performance counters. *Applied Soft Computing*, 49:1162–1174, 2016.
- [10] Ye Dayong, Zhu Tianqing, He Feng, Liu Bo, Xue Minhui, and Zhou Wanlei. Cross-modal prompt inversion: Unifying threats to text and image generative AI models. In *34th USENIX Security Symposium (USENIX Security 25)*. USENIX Association, July 2025.
- [11] Wenxin Ding, Cathy Y. Li, Shawn Shan, Ben Y. Zhao, and Haitao Zheng. Understanding implosion in text-to-image generative models. In *Proceedings of the 2024 on ACM SIGSAC Conference on Computer and Communications Security, CCS '24*, page 1211–1225, New York, NY, USA, 2024. Association for Computing Machinery.
- [12] Zhenbang Du, Wei Feng, Haohan Wang, Yaoyu Li, Jingsen Wang, Jian Li, Zheng Zhang, Jingjing Lv, Xin Zhu, Junsheng Jin, Junjie Shen, Zhangang Lin, and Jingping Shao. Towards reliable advertising image generation using human feedback. In Aleš Leonardis, Elisa Ricci, Stefan Roth, Olga Russakovsky, Torsten Sattler, and Gül Varol, editors, *Computer Vision – ECCV 2024*, pages 399–415, Cham, 2025. Springer Nature Switzerland.
- [13] Abdelrahman Eldesokey and Peter Wonka. Build-a-scene: Interactive 3d layout control for diffusion-based image generation. In *The Thirteenth International Conference on Learning Representations*, 2025.
- [14] Patrick Esser, Sumith Kulal, Andreas Blattmann, Rahim Entezari, Jonas Müller, Harry Saini, Yam Levi, Dominik Lorenz, Axel Sauer, Frederic Boesel, Dustin Podell, Tim Dockhorn, Zion English, Kyle Lacey, Alex Goodwin, Yannik Marek, and Robin Rombach. Scaling rectified flow transformers for high-resolution image synthesis, 2024.
- [15] Fernando A. Fardo, Victor H. Conforto, Francisco C. de Oliveira, and Paulo S. Rodrigues. A formal evaluation of psnr as quality measurement parameter for image segmentation algorithms, 2016.
- [16] Yifan Gao, Zihang Lin, Chuanbin Liu, Min Zhou, Tiezheng Ge, Bo Zheng, and Hongtao Xie. Postermaker: Towards high-quality product poster generation with accurate text rendering. In *Proceedings of the IEEE/CVF Conference on Computer Vision and Pattern Recognition (CVPR)*, pages 8083–8093, June 2025.
- [17] Waris Gill, Mohamed Elidrisi, Pallavi Kalapatapu, Ammar Ahmed, Ali Anwar, and Muhammad Ali Gulzar. MeanCache: User-centric semantic caching for LLM web services, 2025.
- [18] Chongye Guo, Jinhua Fu, Junfeng Fang, Kun Wang, and Guorui Feng. Redediting: Relationship-driven precise backdoor poisoning on text-to-image diffusion models, 2025.
- [19] Jonathan Ho, Ajay Jain, and Pieter Abbeel. Denoising diffusion probabilistic models. In *Proceedings of the 34th International Conference on Neural Information Processing Systems, NIPS '20*, Red Hook, NY, USA, 2020. Curran Associates Inc.
- [20] Gal Horowitz, Eyal Ronen, and Yuval Yarom. Spec-o-Scope: Cache probing at cache speed. In *Proceedings of the 2024 on ACM SIGSAC Conference on Computer and Communications Security, CCS '24*, page 109–123, New York, NY, USA, 2024. Association for Computing Machinery.
- [21] Huayang Huang, Xiangye Jin, Jiaxu Miao, and Yu Wu. Implicit bias injection attacks against text-to-image diffusion models, 2025.
- [22] Zehuan Huang, Yuan-Chen Guo, Xingqiao An, Yunhan Yang, Yangguang Li, Zi-Xin Zou, Ding Liang, Xihui Liu, Yan-Pei Cao, and Lu Sheng. Midi: Multi-instance diffusion for single image to 3d scene generation. In *Proceedings of the IEEE/CVF Conference on Computer Vision and Pattern Recognition (CVPR)*, pages 23646–23657, June 2025.
- [23] Sangwon Jang, June Suk Choi, Jaehyeong Jo, Kimin Lee, and Sung Ju Hwang. Silent branding attack: Trigger-free data poisoning attack on text-to-image diffusion models. *arXiv preprint arXiv:2503.09669*, 2025.
- [24] Tushar M. Jois, Gabrielle Beck, and Gabriel Kaptchuk. Pulsar: Secure steganography for diffusion models. In *Proceedings of the 2024 on ACM SIGSAC Conference on Computer and Communications Security, CCS '24*, page 4703–4717, New York, NY, USA, 2024. Association for Computing Machinery.
- [25] Tejal Joshi, Aarya Kawalay, Anvi Jamkhande, and Amit Joshi. Hybrid deep learning model for multiple cache side channel attacks detection: A comparative analysis, 2025.
- [26] Mehmet Kayaalp, Nael Abu-Ghazaleh, Dmitry Ponomarev, and Aamer Jaleel. A high-resolution side-channel attack on last-level cache. In *Proceedings of the 53rd Annual Design Automation Conference, DAC '16*, New York, NY, USA, 2016. Association for Computing Machinery.
- [27] Michael Kurth, Ben Gras, Dennis Andriess, Cristiano Giuffrida, Herbert Bos, and Kaveh Razavi. NetCAT: Practical cache attacks from the network. In *2020 IEEE Symposium on Security and Privacy (SP)*, pages 20–38, 2020.
- [28] Black Forest Labs. Flux. <https://github.com/black-forest-labs/flux>, 2024.
- [29] Black Forest Labs, Stephen Batifol, Andreas Blattmann, Frederic Boesel, Saksham Consul, Cyril Digne, Tim Dockhorn, Jack English, Zion English, Patrick Esser, Sumith Kulal, Kyle Lacey, Yam Levi, Cheng Li, Dominik Lorenz, Jonas Müller, Dustin Podell, Robin Rombach, Harry Saini, Axel Sauer, and Luke Smith. Flux.1 kontext: Flow matching for in-context image generation and editing in latent space, 2025.
- [30] Jiaying Li, Chi Xu, Feng Wang, Isaac M von Riedemann, Cong Zhang, and Jiangchuan Liu. Scalm: Towards semantic caching for automated chat services with large language models, 2024.
- [31] Xinfeng Li, Yuchen Yang, Jiangyi Deng, Chen Yan, Yanjiao Chen, Xiaoyu Ji, and Wenyan Xu. SafeGen: Mitigating sexually explicit content generation in text-to-image models. In *Proceedings of the 2024 on ACM SIGSAC Conference on Computer and Communications Security*,

- CCS '24, page 4807–4821, New York, NY, USA, 2024. Association for Computing Machinery.
- [32] Fangfei Liu, Yuval Yarom, Qian Ge, Gernot Heiser, and Ruby B. Lee. Last-level cache side-channel attacks are practical. In *2015 IEEE Symposium on Security and Privacy*, pages 605–622, 2015.
- [33] Sihang Liu, Suraj Kanniwadi, Martin Schwarzl, Andreas Kogler, Daniel Gruss, and Samira Khan. Side-Channel attacks on optane persistent memory. In *32nd USENIX Security Symposium (USENIX Security 23)*, pages 6807–6824, Anaheim, CA, August 2023. USENIX Association.
- [34] Zhibo Liu, Yuanyuan Yuan, Yanzuo Chen, Sihang Hu, Tianxiang Li, and Shuai Wang. Deepcache: Revisiting cache side-channel attacks in deep neural networks executables. In *Proceedings of the 2024 on ACM SIGSAC Conference on Computer and Communications Security, CCS '24*, page 4495–4508, New York, NY, USA, 2024. Association for Computing Machinery.
- [35] Jian Ma, Yonglin Deng, Chen Chen, Nanyang Du, Haonan Lu, and Zhenyu Yang. GlyphDraw2: Automatic generation of complex glyph posters with diffusion models and large language models. *Proceedings of the AAAI Conference on Artificial Intelligence*, 39(6):5955–5963, Apr. 2025.
- [36] Lukas Maar, Jonas Juffinger, Thomas Steinbauer, Daniel Gruss, and Stefan Mangard. Kernelsnitch: Side-channel attacks on kernel data structures. In *Network and Distributed System Security Symposium (NDSS) 2025*, February 2025. Network and Distributed System Security Symposium 2025 : NDSS 2025, NDSS 2025 ; Conference date: 23-02-2025 Through 28-02-2025.
- [37] Aqib Mahfuz, Georgia Channing, Mark van der Wilk, Philip Torr, Fabio Pizzati, and Christian Schroeder de Witt. Psyduck: Training-free steganography for latent diffusion, 2025.
- [38] Meta. Introducing Meta Llama 3: The most capable openly available LLM to date. <https://ai.meta.com/blog/meta-llama-3/>, 2024.
- [39] Ramaswami Mohandoss. Context-based semantic caching for Llm applications. In *2024 IEEE Conference on Artificial Intelligence (CAI)*, pages 371–376, 2024.
- [40] Ron Mokady, Amir Hertz, and Amit H. Bermano. Clipcap: Clip prefix for image captioning, 2021.
- [41] Maria Mushtaq, Ayaz Akram, Muhammad Khuram Bhatti, Maham Chaudhry, Vianney Lapotre, and Guy Gogniat. NIGHTS-WATCH: a cache-based side-channel intrusion detector using hardware performance counters. In *Proceedings of the 7th International Workshop on Hardware and Architectural Support for Security and Privacy, HASP '18*, New York, NY, USA, 2018. Association for Computing Machinery.
- [42] Maria Mushtaq, Ayaz Akram, Muhammad Khuram Bhatti, Maham Chaudhry, Muneeb Yousaf, Umer Farooq, Vianney Lapotre, and Guy Gogniat. Machine learning for security: The case of side-channel attack detection at run-time. In *2018 25th IEEE International Conference on Electronics, Circuits and Systems (ICECS)*, pages 485–488, 2018.
- [43] Ali Naseh, Jaechul Roh, Eugene Bagdasarian, and Amir Houmansadr. Backdooring bias (b^2) into stable diffusion models. In *34th USENIX Security Symposium (USENIX Security 25)*. USENIX Association, July 2025.
- [44] OpenAI. Dalle 3 system card. https://cdn.openai.com/papers/DALL_E_3_System_Card.pdf, 2023.
- [45] Maxime Oquab, Timothée Darcet, Theo Moutakanni, Huy V. Vo, Marc Szafraniec, Vasil Khalidov, Pierre Fernandez, Daniel Haziza, Francisco Massa, Alaaeldin El-Nouby, Russell Howes, Po-Yao Huang, Hu Xu, Vasu Sharma, Shang-Wen Li, Wojciech Galuba, Mike Rabbat, Mido Assran, Nicolas Ballas, Gabriel Synnaeve, Ishan Misra, Herve Jegou, Julien Mairal, Patrick Labatut, Armand Joulin, and Piotr Bojanowski. DINOv2: Learning robust visual features without supervision, 2023.
- [46] Zhuoshi Pan, Yuguang Yao, Gaowen Liu, Bingquan Shen, H. Vicky Zhao, Ramana Rao Kompella, and Sijia Liu. From trojan horses to castle walls: Unveiling bilateral data poisoning effects in diffusion models. In A. Globerson, L. Mackey, D. Belgrave, A. Fan, U. Paquet, J. Tomczak, and C. Zhang, editors, *Advances in Neural Information Processing Systems*, volume 37, pages 82265–82295. Curran Associates, Inc., 2024.
- [47] Yinyin Peng, Yaofei Wang, Donghui Hu, Kejiang Chen, Xianjin Rong, and Weiming Zhang. Ldstega: Practical and robust generative image steganography based on latent diffusion models. In *Proceedings of the 32nd ACM International Conference on Multimedia, MM '24*, page 3001–3009, New York, NY, USA, 2024. Association for Computing Machinery.
- [48] Pinecone. Making stable diffusion faster with intelligent caching. <https://www.pinecone.io/learn/faster-stable-diffusion/>, 2023.
- [49] Alec Radford, Jong Wook Kim, Chris Hallacy, Aditya Ramesh, Gabriel Goh, Sandhini Agarwal, Girish Sastry, Amanda Askell, Pamela Mishkin, Jack Clark, Gretchen Krueger, and Ilya Sutskever. Learning transferable visual models from natural language supervision. In Marina Meila and Tong Zhang, editors, *Proceedings of the 38th International Conference on Machine Learning*, volume 139 of *Proceedings of Machine Learning Research*, pages 8748–8763. PMLR, 18–24 Jul 2021.
- [50] Alec Radford, Jeff Wu, Rewon Child, David Luan, Dario Amodei, and Ilya Sutskever. Language models are unsupervised multitask learners. In *OpenAI*, 2019.
- [51] Runpod. Runpod: The cloud built for AI. <https://www.runpod.io/>, 2025.
- [52] Majid Sabbagh, Yunsu Fei, Thomas Wahl, and A. Adam Ding. SCADET: a side-channel attack detection tool for tracking prime+probe. In *Proceedings of the International Conference on Computer-Aided Design, ICCAD '18*, New York, NY, USA, 2018. Association for Computing Machinery.
- [53] Chitwan Saharia, William Chan, Saurabh Saxena, Lala Li, Jay Whang, Emily L Denton, Kamyar Ghasemipour, Raphael Gontijo Lopes, Burcu Karagol Ayan, Tim Salimans, Jonathan Ho, David J Fleet, and Mohammad Norouzi. Photorealistic text-to-image diffusion models with deep language understanding. In S. Koyejo, S. Mohamed, A. Agarwal, D. Belgrave, K. Cho, and A. Oh, editors, *Advances in Neural Information Processing Systems*, volume 35, pages 36479–36494. Curran Associates, Inc., 2022.
- [54] Michael Schwarz, Martin Schwarzl, Moritz Lipp, Jon Masters, and Daniel Gruss. NetSpectre: Read arbitrary memory over network. In *Computer Security – ESORICS 2019: 24th European Symposium on Research in Computer Security, Luxembourg, September 23–27, 2019, Proceedings, Part I*, page 279–299, Berlin, Heidelberg, 2019. Springer-Verlag.
- [55] Martin Schwarzl, Erik Kraft, Moritz Lipp, and Daniel Gruss. Remote memory-deduplication attacks. In *29th Annual Network and Distributed System Security Symposium (NDSS)*. The Internet Society, 2022.
- [56] Shawn Shan, Wenxin Ding, Josephine Passananti, Stanley Wu, Haitao Zheng, and Ben Y. Zhao. Nightshade: Prompt-specific poisoning attacks on text-to-image generative models. In *2024 IEEE Symposium on Security and Privacy (SP)*, pages 807–825, 2024.
- [57] Shawn Shan, Wenxin Ding, Josephine Passananti, Stanley Wu, Haitao Zheng, and Ben Y. Zhao. Nightshade: Prompt-specific poisoning attacks on text-to-image generative models. In *2024 IEEE Symposium on Security and Privacy (SP)*, pages 807–825, 2024.
- [58] Xinyue Shen, Yiting Qu, Michael Backes, and Yang Zhang. Prompt stealing attacks against Text-to-Image generation models. In *33rd USENIX Security Symposium (USENIX Security 24)*, pages 5823–5840, Philadelphia, PA, August 2024. USENIX Association.
- [59] Desen Sun, Henry Tian, Tim Lu, and Sihang Liu. FlexCache: Flexible approximate cache system for video diffusion, 2024.
- [60] Mingze Sun, Junhao Chen, Juntong Dong, Yurun Chen, Xinyu Jiang, Shiwei Mao, Puhua Jiang, Jingbo Wang, Bo Dai, and Ruqi Huang. Drive: Diffusion-based rigging empowers generation of versatile and

- expressive characters. In *Proceedings of the IEEE/CVF Conference on Computer Vision and Pattern Recognition (CVPR)*, pages 21170–21180, June 2025.
- [61] Zekun Sun, Zijian Liu, Shouling Ji, Chenhao Lin, and Na Ruan. Pre-tender: Universal active defense against diffusion finetuning attacks. In *The 34th USENIX Security Symposium*, 2025.
- [62] Mohammadkazem Taram, Ashish Venkat, and Dean Tullsen. Packet chasing: Spying on network packets over a cache side-channel. In *2020 ACM/IEEE 47th Annual International Symposium on Computer Architecture (ISCA)*, pages 721–734, 2020.
- [63] Corban Villa, Shujaat Mirza, and Christina Pöpper. Exposing the guardrails: Reverse-engineering and jailbreaking safety filters in dall-e text-to-image pipelines. In *34th USENIX Security Symposium (USENIX Security 25)*. USENIX Association, July 2025.
- [64] Junpeng Wan, Yanxiang Bi, Zhe Zhou, and Zhou Li. Meshup: Stateless cache side-channel attack on cpu mesh. In *2022 IEEE Symposium on Security and Privacy (SP)*, pages 1506–1524, 2022.
- [65] Alan Wang, Boru Chen, Yingchen Wang, Christopher W. Fletcher, Daniel Genkin, David Kohlbrenner, and Riccardo Paccagnella. Peek-a-walk: Leaking secrets via page walk side channels. In *2025 IEEE Symposium on Security and Privacy (SP)*, pages 3534–3548, 2025.
- [66] Bingyuan Wang, Qifeng Chen, and Zeyu Wang. Diffusion-based visual art creation: A survey and new perspectives. *ACM Comput. Surv.*, 57(10), May 2025.
- [67] Haonan Wang, Qianli Shen, Yao Tong, Yang Zhang, and Kenji Kawaguchi. The stronger the diffusion model, the easier the backdoor: Data poisoning to induce copyright breaches without adjusting finetuning pipeline. In *Forty-first International Conference on Machine Learning*, 2024.
- [68] Peiran Wang, Qiyu Li, Longxuan Yu, Ziyao Wang, Ang Li, and Haojian Jin. Moderator: Moderating text-to-image diffusion models through fine-grained context-based policies. In *Proceedings of the 2024 on ACM SIGSAC Conference on Computer and Communications Security, CCS '24*, page 1181–1195, New York, NY, USA, 2024. Association for Computing Machinery.
- [69] Xiyu Wang, Yufei Wang, Satoshi Tsutsui, Weisi Lin, Bihan Wen, and Alex Kot. Evolving storytelling: Benchmarks and methods for new character customization with diffusion models. In *Proceedings of the 32nd ACM International Conference on Multimedia, MM '24*, page 3751–3760, New York, NY, USA, 2024. Association for Computing Machinery.
- [70] Zijie J. Wang, Evan Montoya, David Munechika, Haoyang Yang, Benjamin Hoover, and Duen Horng Chau. DiffusionDB: A large-scale prompt gallery dataset for text-to-image generative models. In Anna Rogers, Jordan Boyd-Graber, and Naoaki Okazaki, editors, *Proceedings of the 61st Annual Meeting of the Association for Computational Linguistics (Volume 1: Long Papers)*, pages 893–911, Toronto, Canada, July 2023. Association for Computational Linguistics.
- [71] Yixin Wu, Ning Yu, Michael Backes, Yun Shen, and Yang Zhang. On the proactive generation of unsafe images from text-to-image models using benign prompts. *arXiv preprint arXiv:2310.16613*, 2023.
- [72] Yurong Wu, Fangwen Mu, QiuHong Zhang, Jinjing Zhao, Xinrun Xu, Lingrui Mei, Yang Wu, Lin Shi, Junjie Wang, Zhiming Ding, and Yiwei Wang. Vulnerability of text-to-image models to prompt template stealing: A differential evolution approach. In Wanxiang Che, Joyce Nabende, Ekaterina Shutova, and Mohammad Taher Pilehvar, editors, *Findings of the Association for Computational Linguistics: ACL 2025*, pages 16903–16916, Vienna, Austria, July 2025. Association for Computational Linguistics.
- [73] Yuchen Xia, Divyam Sharma, Yichao Yuan, Souvik Kundu, and Nishil Talati. MoDM: Efficient serving for image generation via mixture-of-diffusion models. In *Proceedings of the 31st ACM International Conference on Architectural Support for Programming Languages and Operating Systems, Volume 1 (ASPLOS '26)*, Pittsburgh, PA, USA, March 2026. Association for Computing Machinery.
- [74] Yuanbo Yang, Jiahao Shao, Xinyang Li, Yujun Shen, Andreas Geiger, and Yiyi Liao. Prometheus: 3D-aware latent diffusion models for feed-forward text-to-3D scene generation. In *Proceedings of the IEEE/CVF Conference on Computer Vision and Pattern Recognition (CVPR)*, pages 2857–2869, June 2025.
- [75] Yuval Yarom and Katrina Falkner. FLUSH+RELOAD: A high resolution, low noise, L3 cache side-channel attack. In *23rd USENIX Security Symposium (USENIX Security 14)*, pages 719–732, San Diego, CA, August 2014. USENIX Association.
- [76] Jiwen Yu, Xuanyu Zhang, Youmin Xu, and Jian Zhang. Cross: Diffusion model makes controllable, robust and secure image steganography. In A. Oh, T. Naumann, A. Globerson, K. Saenko, M. Hardt, and S. Levine, editors, *Advances in Neural Information Processing Systems*, volume 36, pages 80730–80743. Curran Associates, Inc., 2023.
- [77] Jiyong Yu, Aishani Dutta, Trent Jaeger, David Kohlbrenner, and Christopher W. Fletcher. Synchronization storage channels (S2C): Timer-less cache Side-Channel attacks on the apple m1 via hardware synchronization instructions. In *32nd USENIX Security Symposium (USENIX Security 23)*, pages 1973–1990, Anaheim, CA, August 2023. USENIX Association.
- [78] Zihao Yu, Haoyang Li, Fangcheng Fu, Xupeng Miao, and Bin Cui. Accelerating text-to-image editing via cache-enabled sparse diffusion inference. *Proceedings of the AAAI Conference on Artificial Intelligence*, 38(15):16605–16613, Mar. 2024.
- [79] Tianwei Zhang, Yinqian Zhang, and Ruby B. Lee. CloudRadar: A real-time side-channel attack detection system in clouds. In Fabian Monrose, Marc Dacier, Gregory Blanc, and Joaquin Garcia-Alfaro, editors, *Research in Attacks, Intrusions, and Defenses*, pages 118–140, Cham, 2016. Springer International Publishing.
- [80] Yuyang Zhang, Jiahui Wen, Yihui Jin, Ziyou Liang, Run Wang, and Lina Wang. USD: NSFW content detection for text-to-image models via scene graph. In *The 34th USENIX Security Symposium*, 2025.
- [81] Zilliz. Semantic cache for LLMs. fully integrated with LangChain and llama_index. <https://github.com/zilliztech/GPTCache>, 2023.